Spectroscopy of ^{153}Gd and ^{157}Gd using the (p,dγ) reaction

T. J. Ross, R. O. Hughes, J. M. Allmond, C. W. Beausang, C. T. Angell, M. S. Basunia, D. L. Bleuel, J. T. Burke, R. J. Casperson, J. E. Escher, P. Fallon, R. Hatarik, J. Munson, S. Paschalis, M. Petri, L. W. Phair, J. J. Ressler, and N. D. Scielzo

Spectroscopy of ^{153}Gd and ^{157}Gd using the (p,d-γ) reaction

T.J. Ross,[1,2,3] R.O. Hughes,[1,*] J.M. Allmond,[4] C.W. Beausang,[1,†] C.T. Angell,[5,‡]
M.S. Basunia,[6] D.L. Bleuel,[7] J.T. Burke,[7] R.J. Casperson,[7] J.E. Escher,[7] P. Fallon,[6] R. Hatarik,[6]
J. Munson,[5] S. Paschalis,[6,§] M. Petri,[6,§] L.W. Phair,[6] J.J. Ressler,[7] and N.D. Scielzo[7]

[1]*Department of Physics, University of Richmond, Richmond, Virginia, 23173, USA*
[2]*Department of Physics, University of Surrey, Guildford, Surrey, GU2 7JL, UK*
[3]*Department of Chemistry, University of Kentucky, Lexington, Kentucky, 40506, USA*
[4]*JINPA, Oak Ridge National Laboratory, Oak Ridge, Tennessee, 37831, USA*
[5]*Department of Nuclear Engineering, University of California, Berkeley, California, 94720, USA*
[6]*Nuclear Science Division, Lawrence Berkeley National Laboratory, Berkeley, California, 94720, USA*
[7]*Lawrence Livermore National Laboratory, Livermore, California, 94551, USA*
(Dated: October 15, 2014)

Low-spin single quasi-neutron levels in ^{153}Gd and ^{157}Gd have been studied following the ^{154}Gd(p,d-γ)^{153}Gd and ^{158}Gd(p,d-γ)^{157}Gd reactions. A combined Si-telescope and HPGe array was utilized, allowing d-γ and d-γ-γ coincidence measurements. Almost all of the established low-excitation energy, low-spin structures were confirmed in both ^{153}Gd and ^{157}Gd. Several new levels and numerous new γ rays are observed in both nuclei, particularly for E$_x \geq 1$ MeV. Residual effects of a neutron sub-shell closure at $N = 64$ are observed in the form of a large excitation energy gap in the single quasi-neutron level schemes.

PACS numbers: 21.10.Pc, 25.40.Hs

I. INTRODUCTION

The Z $\sim$ 64, N $\sim$ 90 nuclei are at the centre of a region of rapid shape change from vibrational (N $\leq$ 90) to rotational (N $\geq$ 90) character. The even-even nuclei in this region have long been a testing ground for various nuclear models. In contrast, the low-lying structure of the odd-even isotopes in the region remain comparatively unstudied and the majority of the low-spin investigations of these isotopes were carried out over thirty years ago and in the main have not been revisited. More recently several (n,γ) studies have been carried out. A summary of some important low-spin studies of ^{153}Gd and ^{157}Gd is provided in Table I.

Recent studies of ^{153}Sm by Blasi *et al.* [11] and ^{155}Gd by Allmond *et al.* [12] have found discrepancies with previous quasi-neutron level assignments, in particular calling previous $\Delta \ell = 4\hbar$ assignments in the region into question. As a result, previous $\frac{7}{2}^{+}$[404] Nilsson state candidates were reassigned as $\frac{5}{2}^{+}$[402] candidates in both nuclei. In the work of Allmond *et al.*, the combination of particle energy, γ-ray energy and angular momentum transfer measurement utilized proved to be a powerful tool for spectroscopic studies and provided numerous handles not possible with particle or γ-ray measurements alone. The technique can remove some of the ambiguity involved in the combination of these separate studies.

The idea of utilizing particle-γ correlations to gain added spectroscopic information is well understood and has been used since the 1960's [13–15]. With advances in detector technologies over the last decade increased energy *and* angular information can be achieved for both particle and γ-ray detection, see for example references [16–20]. A selection of works in a similar vein to the current work can be found in Refs. [12, 21–27].

Recently, we reported on the effects of the spherical $N = 64$ sub-shell closure on the structure of moderately deformed Gd nuclei with $N \sim 90$. These nuclei were populated via the (p,d) one-neutron pickup reaction and using particle-γ coincidence spectroscopy. The effect was revealed by a large energy gap in the single quasi-neutron level schemes of ^{153,155,157}Gd. The excitation energy of the "gap" increases with neutron number and is suggestive of *decreasing* deformation with increasing N. This is in contrast to the traditional picture expected upon inspection of the intervening even-even nuclei and reveals the shape driving effect of the odd neutron orbitals on the underlying nuclear deformation. In this paper we expand upon these results, providing additional spectroscopic details for ^{153}Gd and ^{157}Gd and comparing to recent results reported for ^{155}Gd [12].

II. EXPERIMENT

The experiment was carried out at the 88-Inch Cyclotron at Lawrence Berkeley National Laboratory. A 25 MeV ($\sim$ 2.5 enA) proton beam was used to study (p,d-γ) and (p,t-γ) reactions on ^{154}Gd and ^{158}Gd targets, [29]. The (p,t) reaction was utilized to populate ^{152}Gd

---

* Current address: Lawrence Livermore National Laboratory, Livermore, California, 94551, USA
† Corresponding author: cbeausan@richmond.edu
‡ Current address: Quantum Beam Science Directorate, Japan Atomic Energy Agency, Tokai, Ibaraki 319-1195, Japan
§ Current address: IKP, TU Darmstadt, 64289 Darmstadt, Germany

TABLE I. A summary of light-ion transfer and (n,γ) studies of ^{153}Gd and ^{157}Gd.

Isotope	Reaction	Author [Ref.]	Year
^{153}Gd, ^{157}Gd	(d,p),(d,t)	P.O. Tjøm et al. [1]	1967
^{153}Gd	(d,t),(^{3}He,α)	G. Løvhøiden et al. [2]	1973
^{153}Gd	(p,t)	G. Løvhøiden et al. [3]	1973
^{153}Gd	(α,n)	J. Rekstad et al. [4]	1981
^{157}Gd	(p,d)	K. Yagi et al. [5]	1969
^{157}Gd	(^{3}He,α)	G. Løvhøiden et al. [6]	1970
^{157}Gd	(d,d')	F. Sterba et al. [7]	1971
^{157}Gd	(t,p)	G. Løvhøiden et al. [8]	1989
^{157}Gd	(n,γ)	J. Kopecky et al. [9]	1993
^{157}Gd	(n,γ)	V. Bondarenko et al. [10]	2003

TABLE II. Statistics for each target and reaction.

Target	^{154}Gd	^{158}Gd
Isotopic Purity [%]	66.53(10)	92.00(10)
$^{A+1}$Gd Content [%]	17.50(10)	-
Thickness [mg/cm^2]	1.01(10)	1.01(10)
Time [hrs]	60	51
$(p,d\gamma)$ events	2.1×10^6	2.44×10^6
$(p,d\gamma\gamma)$ events	2.35×10^5	2.55×10^5
$(p,t\gamma)$ events	6.0×10^5	7.54×10^5
$(p,t\gamma\gamma)$ events	1.56×10^5	2.16×10^5

and ^{156}Gd. The (p,d) reaction was utilized to populate ^{153}Gd and ^{157}Gd, the focus of the present work. Events were written to disk when at least one light ion and one γ ray were detected in coincidence. A summary of some details concerning the experiment and targets is provided in Table II.
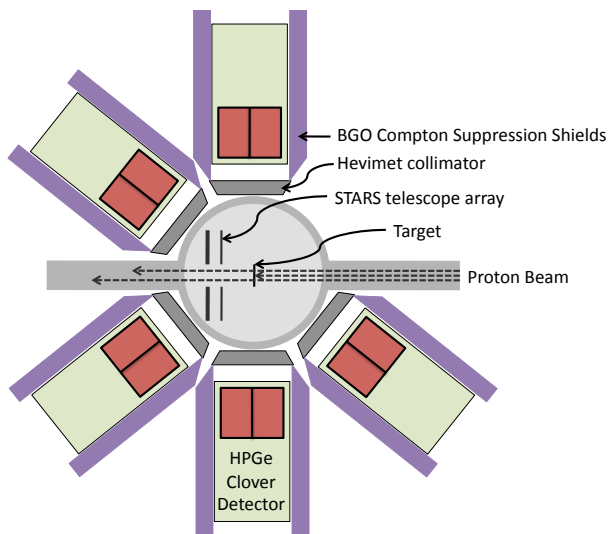

FIG. 1. (Color online.) The experimental setup, described in the text.

A schematic of the experimental setup is shown in Fig. 1. Outgoing light ions were detected using the Silicon Telescope Array for Reaction Studies (STARS) [18]. STARS consists of two Micron S2 silicon annular detectors [30] arranged in a telescope formation. The telescope arrangement allows particle identification utilizing the characteristic energy deposition of the different mass particles. The excitation energy of the residual nucleus can be reconstructed from the energy of the outgoing light ion. The segmentation of the the silicon detector gives the angular distribution of the outgoing light ions, and thus a measurement of the transferred angular momentum. In this experiment, the angular acceptance of the array was between $\sim 33°$ and $\sim 55°$ with respect to the beam axis.

The silicon detectors were energy calibrated at the beginning and end of the experiment using a ^{226}Ra α-emitting source and each had an intrinsic resolution on the order of 150 keV at full width half maximum (FWHM). Additional in-beam calibrations were made using levels directly populated in the reaction. Several energy corrections were made on an event-by-event basis to correct for light-ion energy loss in dead-layers in the silicon detectors (0.1 μm aluminum on the front surface and 0.3 μm gold on the reverse). Detected particles were also subject to a ray trace using segmentation in the ΔE-E telescope to confirm that they originate from the target position. Due to these corrections, the angular spread of detected deuterons, and the addition of the measured energies from the separate detectors, the in-beam telescope resolution was FWHM ~ 360 keV.

Gamma rays were measured in coincidence with the detected particles using the LIvermore BERkeley Array for Collaborative Experiments (LIBERACE) [18]. For this experiment, the LIBERACE array consisted of five HPGe clover detectors which were arranged around the STARS chamber as shown in Fig. 1. All detectors were in the same plane. Two detectors were placed at 90°, two at forward angles of 50° and one at a backward angle of 130°. An energy resolution of ~ 1.9 keV FWHM was achieved at 200 keV and ~ 4.5 keV FWHM was achieved at ~ 1.5 MeV. The photopeak efficiency of the array was calibrated using ^{152}Eu, ^{133}Ba and ^{207}Bi sources. The efficiency of the array peaked at 2.6% at ~ 200 keV and drops to 1.25% at ~ 1 MeV. Internal conversion coefficients were calculated using BrIcc, [31] where experimental values were not available.

III. THE ^{154}Gd(p,d-γ)^{153}Gd REACTION.

The projection of deuterons in coincidence with γ rays following the ^{154}Gd(p,d-γ)^{153}Gd reaction is shown in Fig. 2 (a) (dashed spectrum). Up to the neutron separation energy, S$_n$, at 6.25 MeV, this projection represents the ensemble of states populated in ^{153}Gd which decay via γ-ray emission. The large "peak", between 0 and 0.5 MeV, corresponds to a series of low lying states in ^{153}Gd which are directly populated by the (p,d) reac-

tion. The second "peak" at ~ 1.5 MeV corresponds to a second set of states in ^{153}Gd which are also directly populated. Above this energy a continuum of states is populated up to the neutron-separation energy. Above the neutron-separation energy, neutron emission begins to dominate. Gamma rays detected in coincidence with deuterons from this region are predominantly from ^{152}Gd following the ^{154}Gd(p,dn)^{152}Gd reaction.
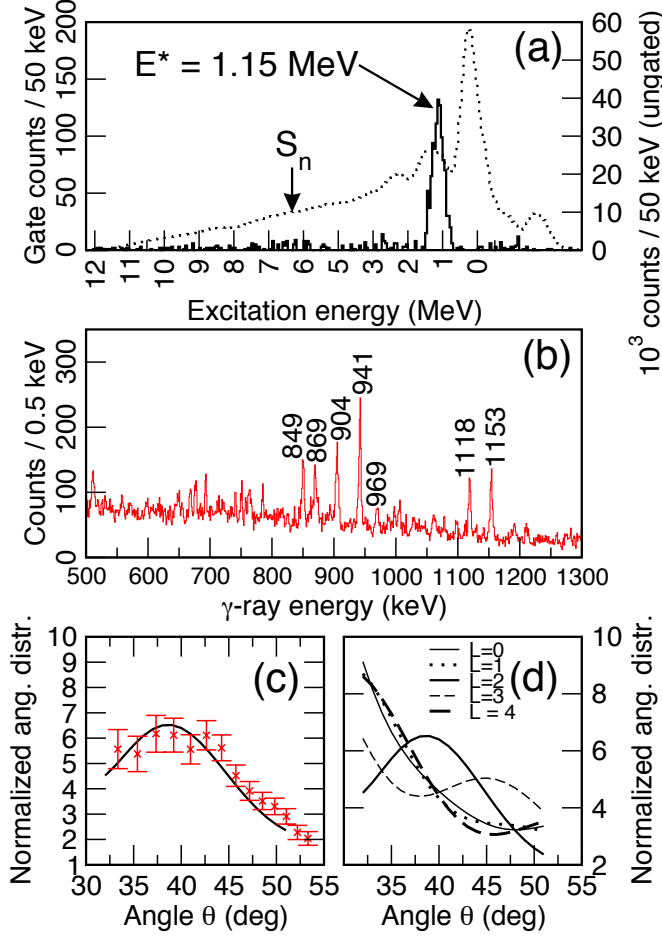

FIG. 2. (Color online.) Measured observables from the ^{154}Gd(p,dγ)^{153}Gd reaction. (a) Deuterons in coincidence with the 941 keV γ ray (solid spectrum). Total deuteron energy projection (dashed spectrum). (b) Gamma rays in coincidence with excitation energies of $1 \leq E^* \leq 1.3$ MeV. (c) Angular distribution of deuterons in coincidence with γ rays of 939 keV $\leq E_\gamma \leq$ 943 keV and 1000 keV $\leq E_{deuteron} \leq$ 1300 keV. (d) The DWBA calculations for angular momentum transfers $\Delta\ell = 0, 1, 2$ and $3\ \hbar$. This figure first appeared in Ref. [28] and is reproduced for completeness.

As shown in Table II, the ^{154}Gd target contained a considerable ($\sim 18\%$) contaminant of ^{155}Gd. One clear effect of this contamination is the presence of particles with $E \leq 0$ MeV in Fig. 2 (a). Data associated with the (p,d) reaction on ^{155}Gd is offset from the data of interest due to the different ground-state Q-values of the two reactions and can be distinguished using particle-γ
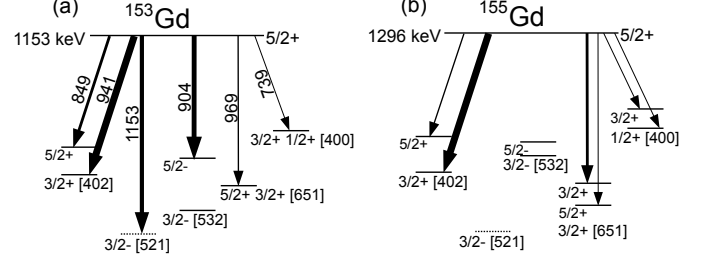
coincidences.

FIG. 3. (a) Partial decay scheme of the newly assigned 1153 keV, $\frac{5}{2}^+$ level in ^{153}Gd. (b) Similarly showing the six most intense transitions from the 1296 keV level in ^{155}Gd, see Ref. [12].

A. The particle-γ coincidence technique.

The power of the γ-ray coincidence technique is demonstrated by the solid spectrum in Fig. 2 (a), which shows the deuterons in coincidence with a γ ray which deexcites a directly populated level in ^{153}Gd. In this case, a gate is placed upon a previously unobserved γ ray, $E_\gamma = $ 941 keV. The deuteron peak in Fig. 2 (a) corresponds to the energy of the level which the 941 keV transition depopulates (1.15 MeV in this case). A back-gate on this excitation energy region returns γ rays which decay from levels with approximately the same excitation energy. The γ rays in coincidence with deuterons whose energies correspond to the excitation energy region 1 - 1.3 MeV are shown in Fig. 2 (b). As expected, the 941 keV γ ray is prominent. The other γ rays in Fig. 2 (b) correspond to other decays associated with the same level, decays from other levels in the selected excitation energy region, or to decays further down the level scheme, most of which are well established. Combining the measurement of initial excitation energy and our knowledge of the low-lying level scheme, the observed γ rays typically only build upon the low-lying level scheme in one particular arrangement and allow a precise measurement of the excitation energy of the new level, 1152.9 ± 0.1 keV in this case. In Fig. 3 (a) the decay scheme of the 1153 keV level is shown. The six decays are all newly observed and can be seen in Fig. 2 (b).

Information about the spin of the level can be gleaned from the angular distribution of the deuterons in the silicon detectors. By placing a coincidence requirement upon both a particle energy and a γ-ray energy, very high deuteron selectivity can be achieved. In Fig. 2 (c) the angular distribution of deuterons in coincidence with both the 941 keV γ ray and the excitation energy region, 1000–1300 keV, is shown and compared to a distorted wave born approximation (DWBA) calculation for $\Delta\ell = 2\ \hbar$ transfer. Calculations for ℓ-transfers of 0–3 $\hbar$ are shown in Fig. 2 (d). The deuterons which populate the

TABLE III. The optical-model parameters used in calculating the (p,d) angular distributions. These parameters were obtained from references [33, 34]. Notation used is in accordance with the notation of reference [35].

Reaction / Particle	V_{SO}	r_{SO}	a_{SO}	V	r_0	a_0	W_d	R_d	a_d	Reference
(p,d) / p	12.0	1.10	0.70	55.7	1.20	0.70	11.3	1.25	0.70	Fleming *et al* [33] param. set "D"
(p,d) / d	-	-	-	100.7	1.15	0.81	18.9	1.34	0.68	Perey and Perey [34] param. set "B"

1153 keV state clearly best resemble a $\Delta\ell = 2\ \hbar$ transfer. This allows a J^π assignment of $\frac{3}{2}^+$ or $\frac{5}{2}^+$ to be made for the 1153 keV level. It should be noted that some of the DWBA curves are very similar over the angular range of the silicon detector array and that such unambiguous ℓ-transfer assignments are not always possible.

The DWBA calculations were carried out with the DWUCK4 code [32] using the optical model parameters summarized in Table III. Further details can be found in Ref. [26].

B.   Results in ^{153}Gd.

Analysis techniques similar to those described above are used to assign other previously unobserved transitions. A summary of the newly observed γ rays in ^{153}Gd, the levels to which they are assigned, and the measured angular distributions for those levels, is presented in Table IV.

The level scheme for ^{153}Gd is shown in Fig. 4 where levels are labelled by their spins, parities and excitation energies, and have been separated according to their assigned quasiparticle configuration. For clarity the γ rays connecting these levels are not shown in Fig. 4. The majority of these structures have been established by a number of transfer reaction studies mostly dating from the 1970's and 80's, see Table I. The current study is in agreement with these studies. Levels with new assignments and/or γ rays are indicated in Fig. 4 by dashed lines. To aid in the interpretation of these levels the evolution of the single quasi-neutron orbitals, as a function of deformation is shown in Fig. 5. While this diagram reflects a relatively simple calculation, the general trends serve as a valuable tool in interpreting the nuclear structure.

A summary of the population yields of levels following the ^{154}Gd(p,d-γ)^{153}Gd reaction is presented in Table V. These yields are expressed relative to the most intensely populated level, the $\frac{3}{2}^+$ level at 212 keV, which is given $I_{rel} = 100$. Yields are determined from the measured area of the direct population deuteron peak in a spectrum gated by a gamma ray depopulating the level of interest. The measured areas are further corrected for the gamma-ray detection efficiency, internal conversion and gamma-ray branching ratios. If possible, the measured yields were cross checked by using several deuteron spectra selected by different gamma-ray gates. It should be noted that no correction is made for the finite solid

angle of the silicon telescope and thus these are relative yields measured between 33° and 55° with respect to the beam axis.

The result of most interest is the aforementioned level observed at 1152.9 ± 0.1 keV and its six associated γ-ray decays. A level at approximately this energy has been observed in two previous charged-particle-only studies, both employing the (d,t) reaction. Løvhøiden *et al.* [2] observed a state at 1151 keV and report an angular-momentum transfer of $\Delta\ell = 2$ or $3\ \hbar$. In the study by Tjøm *et al.* [1] a level at 1151 keV was assigned as the $\frac{7}{2}^-$, $\frac{1}{2}^-$ [521] Nilsson configuration.

As mentioned above, the angular distribution of the deuterons populating the 1153 keV state most closely resembles $\Delta\ell = 2\ \hbar$ transfer, see Fig. 2 (c), allowing a J^π assignment of $\frac{3}{2}^+$ or $\frac{5}{2}^+$. The combination of this result and the γ-ray decay paths allows us to unambiguously assign this level as $\frac{5}{2}^+$.

The decay path is similar to the decay path of the $\frac{5}{2}^+$, $\frac{5}{2}^+$ [402] candidate observed by Allmond *et al.* in ^{155}Gd, Fig. 3 (b). The relative population is also in good agreement with that observed for the analog state in ^{155}Gd [12] (it is the third most intensely populated positive parity state). Therefore we assign the $\frac{5}{2}^+$ state as the $\frac{5}{2}^+$, $\frac{5}{2}^+$ [402] Nilsson candidate, see Fig. 5.

A second level with angular-momentum transfer of $\Delta\ell = 2\ \hbar$ is measured at 1117.8 ± 0.2 keV. Several other studies have reported states close to this energy. Løvhøiden *et al.* [2] observed a level at 1116 keV with $\Delta\ell = 2\ \hbar$ transfer following the (d,t) and (^{3}He,α) reactions. In the literature one finds two levels near this energy. The first, at 1118.48 keV, measured by Alikov *et al.* [37] following electron capture on ^{153}Tb, has nine γ-ray decays and was assigned $\frac{3}{2}^+$. The second, at 1118.34 keV, has four associated γ-ray decays and is assigned either $\frac{3}{2}^-$ or $\frac{5}{2}^-$ following the (n,γ) reaction by Spits *et al.* [38].

We observe two of the γ rays previously assigned to the 1118.48 keV level. It is notable that we do not observe the other seven γ rays which were previously associated with this level and which we would expect to observe based upon the their adopted intensities. Based upon the γ-ray decays observed and an angular momentum transfer of 2$\hbar$, we are not able to distinguish between a $\frac{3}{2}^+$ or $\frac{5}{2}^+$ assignment for this level.

A third level is observed at 1474.3 ± 0.4 keV with three associated γ-ray decays which feed known $\frac{9}{2}^+$, $\frac{13}{2}^+$ and $\frac{13}{2}^-$ levels. The angular momentum transferred was not measured in this case due to limited statistics but these

γ-ray decays suggest a high angular momentum transfer. In previous studies using (d,t) and (^{3}He,α) reactions [2] a level was also seen at 1474 keV, but with much higher intensity following the (^{3}He,α) reaction. An angular momentum transfer of $\Delta\ell = 5$ $\hbar$ was assigned. On the basis of this high angular momentum transfer, the state was tentatively assigned as $\frac{11}{2}^-$, $\frac{9}{2}^-$ [514]. The new γ-rays observed in the present work confirm this assignment.

Finally, a level with three new γ-ray decays is found at 1509.5 ± 0.3 keV. The angular distribution of the outgoing deuterons is not clear, although angular momentum transfer of 0, 1 or 4 $\hbar$ can be ruled out and a chi-squared minimization suggests $\Delta\ell = 3$ $\hbar$ transfer. A level was previously observed at this energy by Løvhøiden et $al.$ [2] who tentatively assigned it $\frac{7}{2}^+$, $\frac{7}{2}^+$ [404], based upon a measured $\Delta\ell = 4$ $\hbar$ transfer. Whilst the three γ-ray decays observed in this work do not rule out this assignment, the measured angular distribution is not supportive. We do not make a firm assignment.

TABLE IV. Summary of new γ rays and levels observed in ^{153}Gd. Shown are the excitation energy of the new level ($E_{initial}$), our spin and parity assignment ($J^{\pi}_{initial}$), the γ-ray energy (E_{γ}), and the relative intensities (I_{γ}) of the γ rays depopulating the level. E_{final} and J^{π}_{final} give the energy, spin and parity of the level to which the γ ray decays as established in the nuclear data sheets [36].

| $E_{initial}$ (keV)	$J^{\pi}_{initial}$	$\Delta\ell$	E_{γ} (keV)	I_{γ}	E_{final} NDS (keV)	J^{π}_{final}
1117.8(2)	$\frac{3}{2}^{+}$, $\frac{5}{2}^{+}$	2	868.2(3)	91(8)	249.5538(11)	$\frac{5}{2}^{-}$
			1117.9(2)	100(9)	0.0	$\frac{3}{2}^{-}$
1152.9(1)	$(\frac{5}{2}^{+})$	2	739.82(24)	7(3)	412.8948(11)	$\frac{3}{2}^{+}$
			848.96(15)	42(6)	303.5428(8)	$\frac{5}{2}^{+}$
			903.87(15)	73(7)	249.5538(11)	$\frac{5}{2}^{-}$
			940.71(9)	100(8)	212.0078(8)	$\frac{3}{2}^{+}$
			968.5(4)	15(4)	183.4695(7)	$\frac{5}{2}^{+}$
			1152.88(14)	64(6)	0.0	$\frac{3}{2}^{-}$
1474.3(4)	$(\frac{11}{2}^{-})$	-	1110.3(3)	79(15)	363.448(14)	$\frac{13}{2}^{-}$
			1335.3(8)	47(17)	139.79(15)	$\frac{13}{2}^{+}$
			1379.24(21)	100(15)	95.1736(8)	$\frac{9}{2}^{+}$
1509.5(3)	-	-	1297.8(5)	68(12)	212.0078(8)	$\frac{3}{2}^{+}$
			1416.04(23)	100(13)	93.3426(6)	$\frac{7}{2}^{-}$
			1467.93(16)	85(11)	41.5566(4)	$\frac{5}{2}^{-}$
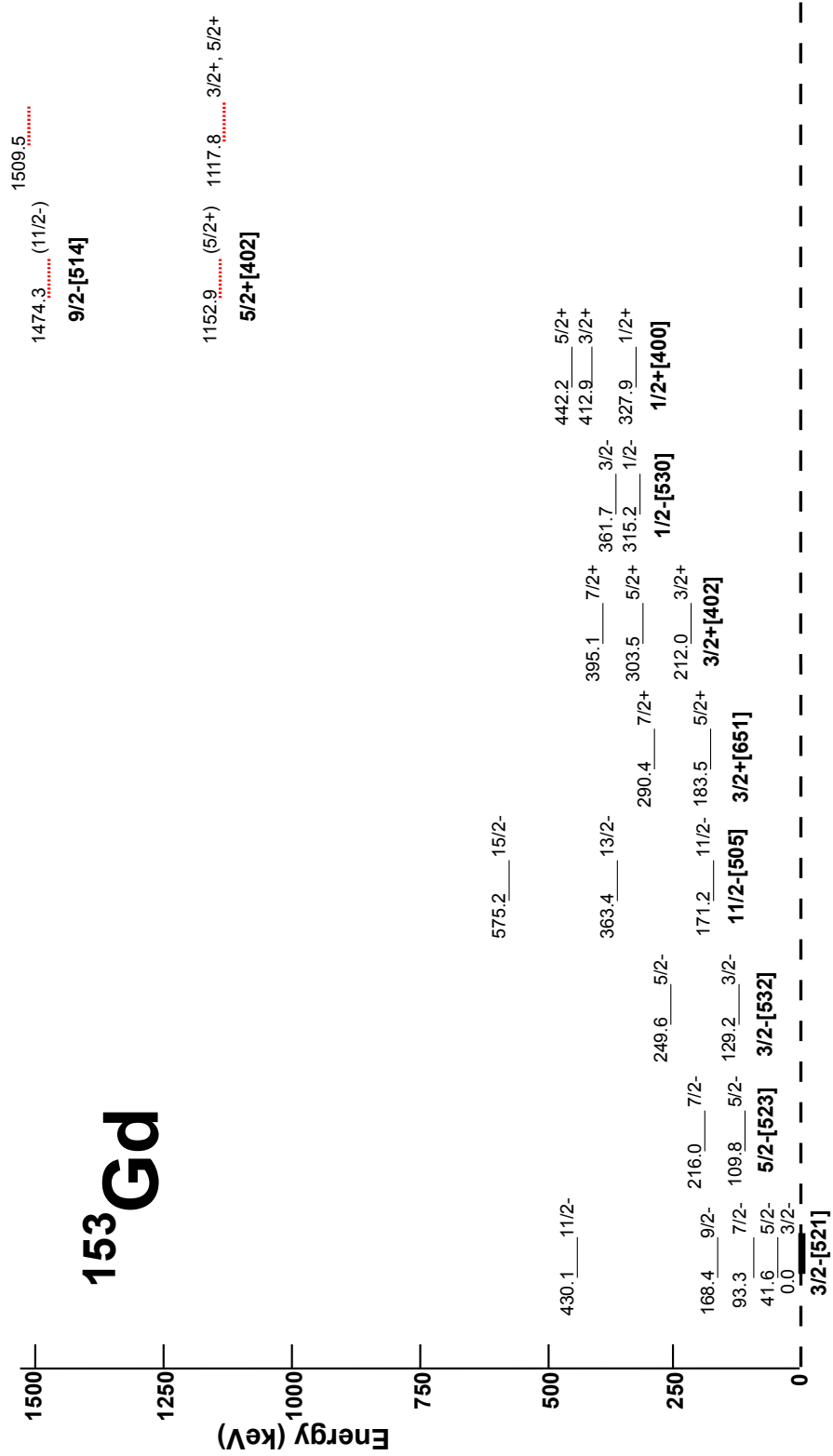
FIG. 4. (Color online.) The ^{153}Gd level scheme, [36], labelled by adopted Nilsson assignment, spin/parity and energy in keV. States with new assignments and/or newly observed γ rays are denoted by dashed lines. For clarity the γ rays connecting these levels are not shown but are presented in Table IV.

TABLE V. Relative population yields from the current work for levels directly populated by the ^{154}Gd(p,d)^{153}Gd reaction. Yields (I_{rel}) are shown relative to the most strongly populated state, the $\frac{3}{2}^+$ at 212 keV. New excitation energy (E^*), spin/parity (J^π) and Nilsson assignments are signified by a star. Other information is from the adopted Nuclear Data Sheets [36]. Selected other states of interest not directly populated by the reaction are shown for completeness and are signified by a dash in the I_{rel} column. Relative yields are measured between $33°$ and $55°$ with respect to the beam axis.

| E^* (keV)	I_{rel}	J^π	$\Omega^\pi[Nn_z\Lambda]$
0.0	-	$\frac{3}{2}^-$	$\frac{3}{2}^-[521]$
41.5566 (4)	-	$\frac{5}{2}^-$	$\frac{3}{2}^-[521]$
94.3426 (6)	-	$\frac{7}{2}^-$	$\frac{3}{2}^-[521]$
109.7560 (7)	27.4(11)	$\frac{5}{2}^-$	$\frac{5}{2}^-[523]$
129.1635 (6)	6.0(14)	$\frac{3}{2}^-$	$\frac{3}{2}^-[532]$
212.0078 (7)	100(3)	$\frac{3}{2}^+$	$\frac{3}{2}^+[402]$
215.9927 (10)	3.6(4)	$\frac{7}{2}^-$	$\frac{5}{2}^-[523]$
219.4426 (11)	7.4(6)	$\frac{9}{2}^-$	$\frac{5}{2}^-[523]$
303.5428 (8)	9.9(11)	$\frac{5}{2}^+$	$\frac{3}{2}^+[402]$
315.1991 (14)	9.3(5)	$\frac{1}{2}^-$	$\frac{1}{2}^-[530]$
327.8525 (12)	88(3)	$\frac{1}{2}^+$	$\frac{1}{2}^+[400]$
333.1681 (17)	3.1(4)	$\frac{9}{2}^-$	$\frac{3}{2}^-[521]$
361.6507 (10)	43(2)	$\frac{3}{2}^-$	$\frac{1}{2}^-[530]$
395.1458 (12)	1.4(4)	$\frac{7}{2}^+$	$\frac{3}{2}^+[402]$
412.8948 (11)	19.4(16)	$\frac{3}{2}^+$	$\frac{1}{2}^+[400]$
436.2710 (15)	5.3(4)	$\frac{1}{2}^-$	$\frac{1}{2}^-[521]$
442.1909 (10)	4.8(8)	$\frac{5}{2}^+$	$\frac{1}{2}^+[400]$
579.125 (3)	5.6(4)	$\frac{7}{2}^-$	$\frac{1}{2}^-[530]$
720.345 (3)	6.4(8)	$\left(\frac{5}{2}^-,\frac{7}{2}^-\right)$	$\frac{1}{2}^-[521]$
945.249 (6)	8.6(11)	$\frac{3}{2}^+$	
1117.8 (2) *	5.3(5)	$\frac{3}{2}^+,\frac{5}{2}^+$ *	
1152.9 (1) *	16.5(18)	$\frac{5}{2}^+$ *	$\frac{5}{2}^+[402]$ *
1474.3 (4) *	6.5(9)	$\frac{11}{2}^-$ *	$\frac{9}{2}^-[514]$ *
1509.5 (3) *	7.1(11)		
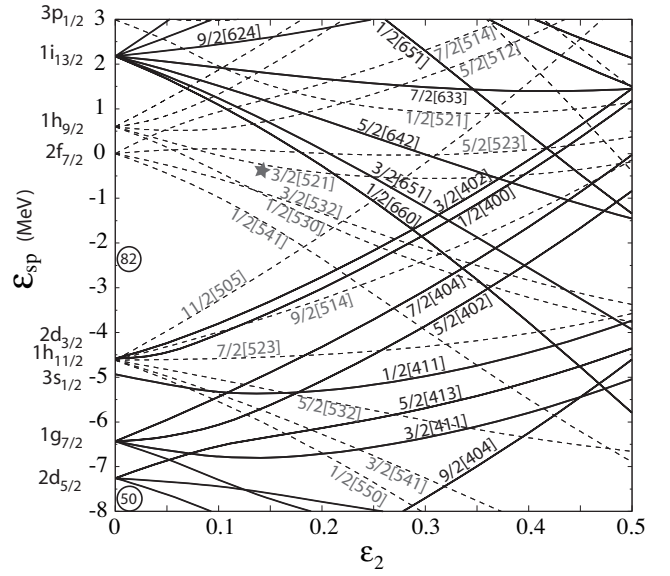
FIG. 5. The Nilsson diagram centered near the N = 91 region. The ground state orbital for ^{153}Gd and ^{157}Gd, $\frac{3}{2}^-$, $\frac{3}{2}^-[521]$, is marked by a star. This figure first appeared in Ref. [12] and is reproduced here for ease of reference.

IV. THE ^{158}Gd(p,d-γ)^{157}Gd REACTION.

A summary of newly observed γ rays and the levels to which they are assigned in ^{157}Gd is provided in Table VI. Whilst some of these seven levels have been previously observed, all twenty-three γ-ray transitions are observed for the first time in this work. Relative population yields for the levels populated in ^{157}Gd in this study (including the newly-observed levels shown in Table VI) are presented in Table VII. Population yields are given relative to the most intensely populated state, the 682 keV $\frac{1}{2}^+$ level, which is given $I_{rel} = 100$. Quasi-particle assignments are also shown in Table VII.

The level scheme of ^{157}Gd is presented in Fig. 6, where the levels are labelled by spins, parities and excitation energies, and have been separated according to their assigned quasiparticle structure [39]. These structures have been primarily established based upon several light-ion transfer reaction studies shown in Table I. We find good agreement with most of the low-lying level scheme established in the literature. Levels with new information are signified by a dashed line in Fig. 6 and will be discussed below.

A. The $\Delta\ell = 2\ \hbar$ states

The levels at 1552 keV, 1589 keV, 1735 keV, and 1825 keV all have an angular momentum transfer consistent with $\Delta\ell = 2\ \hbar$, implying a J^π of either $\frac{3}{2}^+$ or $\frac{5}{2}^+$, Figure 8. Based upon the observed decays to states of known spin and parity (specifically a $\frac{7}{2}^-$ state), the levels at 1552 keV, 1735 keV and 1825 keV can be assigned $J^\pi = \frac{5}{2}^+$. However, the decay of the 1589 keV level cannot distinguish between a $\frac{3}{2}^+$ or $\frac{5}{2}^+$ assignment.

All four levels are potential candidates for the $\frac{5}{2}^+$[402] Nilsson state. In both ^{153}Gd and ^{155}Gd the $\Delta\ell = 2\ \hbar$ state with the strongest population yield above 1 MeV was assigned the $\frac{5}{2}^+$, $\frac{5}{2}^+$[402] configuration. In ^{157}Gd the most intensely populated level is at 1825 keV with $I_{rel} = 14.3$. However, its predominant decay to the $\frac{5}{2}^-$ state at 434 keV is inconsistent with the observed branching ratios of the $\frac{5}{2}^+$[402] candidates in ^{153}Gd and ^{155}Gd (Fig. 3).

An 1825(5) keV level observed in (d,t) reactions in Ref. [1] was previously assigned as the $\frac{7}{2}^+$[404] Nilsson state based upon an apparent $\Delta\ell = 4\ \hbar$ angular momentum transfer. In Ref. [5] a level populated via the (p,d) reaction with angular momentum transfer of $\Delta\ell = 2\ \hbar$ was seen at 1840(20) keV. It is likely that these are in fact the same state observed in the present work at 1825.6 keV. Our $\Delta\ell = 2\ \hbar$ angular momentum transfer measurement for the level rules out the $\frac{7}{2}^+$ assignment of Ref. [1] but is consistent with Ref. [5]. We therefore reassign this state $J^\pi = \frac{5}{2}^+$. This reassignment is consistent with similar mis-assignments of $\frac{7}{2}^+$ states in other isotopes in the region [11, 12].

Although the level at 1589 keV is only populated with approximately a third of the strength of the 1825 keV level, it has a γ-ray decay pattern (Fig. 7) which is much more similar to that of the $\frac{5}{2}^+$[402] level in ^{153}Gd and ^{155}Gd (Figure 3). Due to the ambiguities discussed above no firm assignment of the $\frac{5}{2}^+$[402] orbital can be made in ^{157}Gd.

B. Higher spin states

Six γ-ray transitions are observed to depopulate a level at 1905 keV. The deuteron angular distribution in this case does not allow a spin and parity assignment but the γ-ray decay pattern (Table VI) suggests a high spin state and allows a precise determination of the level energy, 1905.9 (4). In the (^{3}He,α) work by Løvhøiden et al., [6], a level was observed at 1902 $\pm$ 15 keV with an angular momentum transfer of $\Delta\ell = 5\ \hbar$ and the level was assigned as $\frac{11}{2}^-$, $\frac{9}{2}^-$[514]. The 1905 keV level observed in the current work is probably the same. The relative population intensity of the level (4.9) is similar to that of the analogue $\frac{11}{2}^-$, $\frac{9}{2}^-$[514] level in both ^{153}Gd and ^{155}Gd.

The 1906 keV level exhibits decays to both the 427 and 579 keV states, furthermore, our $d-\gamma-\gamma$ indicate a coincidence between the newly observed 1326 keV decay from the 1906 keV level and the previously observed 153 keV decay from the level at 579 keV [10]. Our results therefore support the previous assignment of the 579 keV state as the $\frac{13}{2}^-$ member of the $\frac{11}{2}^-$[505] band [10].

A third high-spin level is observed at 849 keV with a single γ ray, 488.23 keV. The 488 keV γ ray is in coincidence with a 181 keV γ ray which decays from the $\frac{13}{2}^+$ level at 361 keV. The deuteron angular distribution rules out $\Delta\ell = 0$, 1 or 4 $\hbar$ transfer. This level has a low relative population intensity, 3.8. Løvhøiden et al. [6] also observe a state at ~ 850 keV with an angular momentum transfer of $\Delta\ell = 6\ \hbar$ and with a higher cross-section (as might be expected for the (^{3}He,α) reaction).

C. Two re-assignments

Two levels listed in the Data Sheets [39] are very close to each other in excitation energy; the $\frac{1}{2}^+$, $\frac{1}{2}^+$[400] at 682.90 keV and the $\frac{3}{2}^+$, $\frac{3}{2}^+$[651] at 683.233 keV. Both γ rays which were previously associated with the 682.90 keV level (208 keV and 683 keV) are observed and confirmed in the current work. The angular distribution of outgoing deuterons in coincidence with excitation energies of ~ 680 keV and the 208 keV γ ray is best characterized by $\Delta\ell = 0$, 1, 4 $\hbar$ as would be expected for a $\frac{1}{2}^+$ level ($\Delta\ell = 0$).
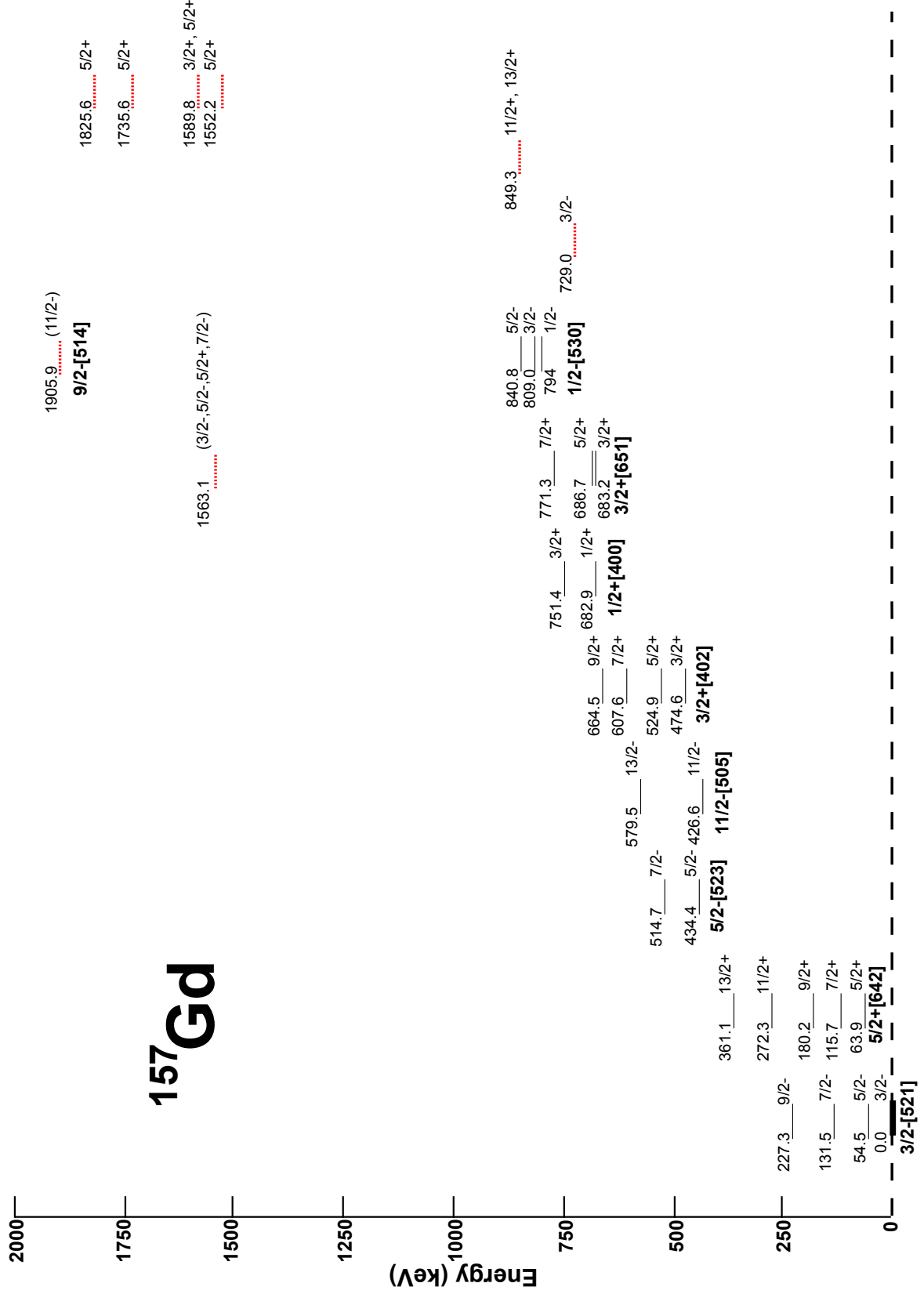
FIG. 6. (Color online.) The ^{157}Gd level scheme, [39], labelled by adopted Nilsson assignment, spin/parity and energy in keV. States with new assignments and/or newly observed γ rays are denoted by dashed lines. For clarity the γ rays connecting these levels are not shown but are presented in Table VI.

TABLE VI. A summary of new levels and γ rays observed in ^{157}Gd. $E_{initial}$ are level energies as measured in this work. $J^\pi_{initial}$ represents the spin and parity of the level. E_γ corresponds to new γ-ray energies for decays from the level $E_{initial}$. I_γ is the relative intensity of the γ ray leaving the level. E_{final} NDS and J^π_{final} gives the excitation energy and spin and parity of the final level as established in the Nuclear Data Sheets, [39].

| $E_{initial}$ (keV)	$J^\pi_{initial}$	$\Delta\ell$	E_γ (keV)	I_γ	E_{final} NDS (keV)	J^π_{final}
849.3(2)	$\frac{11}{2}^+$, $\frac{13}{2}^+$	-	488.23(14)	100(0)	361.10(10)	$\frac{13}{2}^+$
1552.2(2)	$\frac{5}{2}^+$	2	1420.97(18)	95(19)	131.46(9)	$\frac{7}{2}^-$
			1497.30(30)	100(20)	54.533(6)	$\frac{5}{2}^-$
			1552.35(22)	88(17)	0	$\frac{3}{2}^-$
1563.1(6)	$(\frac{3}{2}^-, \frac{5}{2}^-, \frac{5}{2}^+, \frac{7}{2}^-)$	-	1431.8(4)	58(21)	131.46(9)	$\frac{7}{2}^-$
			1507.7(8)	64(25)	54.533(6)	$\frac{5}{2}^-$
			1563.6(6)	100(32)	0	$\frac{3}{2}^-$
1589.8(2)	$\frac{3}{2}^+$, $\frac{5}{2}^+$	2	1064.74(20)	33(6)	524.850(7)	$\frac{5}{2}^+$
			1115.55(16)	100(12)	474.629(6)	$\frac{3}{2}^+$
			1154.87(22)	46(7)	434.426(6)	$\frac{5}{2}^-$
1735.6(2)	$\frac{5}{2}^+$	2,5	984.23(22)	29(7)	751.432(13)	$\frac{3}{2}^+$
			1221.20(30)	31(7)	514.671(8)	$\frac{7}{2}^-$
			1301.13(13)	100(12)	434.426(6)	$\frac{5}{2}^-$
1825.6(1)	$\frac{5}{2}^+$	2	1310.89(15)	37(4)	514.671(8)	$\frac{7}{2}^-$
			1350.86(21)	9.4(19)	474.629(6)	$\frac{3}{2}^+$
			1391.24(6)	100(6)	434.426(6)	$\frac{5}{2}^-$
			1709.8(4)	9(2)	115.717(7)	$\frac{7}{2}^+$
1905.9(4)	$(\frac{11}{2}^-)$	-	1326.6(2)	100(15)	579.46(9)	$\frac{13}{2}^-$
			1478.8(3)	15.5(57)	426.60(5)	$\frac{11}{2}^-$
			1543.6(5)	34(9)	361.10(10)	$\frac{13}{2}^+$
			1632.8(4)	13(5)	272.25(21)	$\frac{11}{2}^+$
			1679.8(5)	56(12)	227.31(5)	$\frac{9}{2}^-$
			1724.9(4)	25(7)	180.229(11)	$\frac{9}{2}^+$
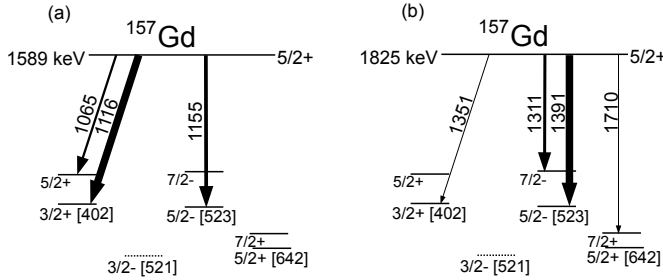
FIG. 7. The decay path of the $\frac{5}{2}^+$[402] candidates in ^{157}Gd.

Only one of the γ rays (619 keV) previously associated with the $\frac{3}{2}^+$[651] level is observed in the current work. The angular distribution of deuterons in coincidence with the 619 keV γ ray (and $\sim$ 680 keV energy region) is also well characterized by $\Delta\ell = 0$, 1, 4 $\hbar$. For a state of spin and parity $\frac{3}{2}^+$, a $\Delta\ell = 2$ $\hbar$ angular distribution is required, which we can rule out in this case. Therefore, due to the measured $\Delta\ell = 0$, 1, 4 $\hbar$ angular distribution

we reassign and associate the entire strength of the 619 keV γ ray with the 682.90 keV, $\frac{1}{2}^+$ state. This makes the $\frac{1}{2}^+$[400] level the most intensely populated state in the current work and yield measurements provided in Table VII are quoted relative to this state.

The level at 729.02 keV ([39]) is measured with a strong relative population intensity of 13.4. Two γ rays are observed depopulating this level; 729 keV to the $\frac{3}{2}^-$ ground state and 674 keV to the $\frac{5}{2}^-$ member of the ground state band. Another γ ray associated with this level (the second most intense decay in the nuclear data sheets [39]), $E_\gamma = 614$ keV, is not observed and can be ruled out. The angular distribution of outgoing deuterons in coincidence with excitation energies of $\sim$ 730 keV and the 729 keV γ ray is best characterized by $\Delta\ell = 0$, 1, 4 $\hbar$, see Fig. 8. On the basis of the two observed γ rays and the measured angular distribution the level is assigned $J^\pi = \frac{1}{2}^-$ or $\frac{3}{2}^-$.

The (p,d) study of Yagi *et al.* also reports a level at 0.70 ± 0.02 MeV, [5], with a measured angular momentum transfer of $\Delta\ell = 1$ $\hbar$. Recent (n,γ) reaction studies assign this level $J^\pi = \frac{3}{2}^-$ [9, 10]. The study by Bon-

TABLE VII. Relative yields for levels directly populated by the ^{158}Gd(p,d)^{157}Gd reaction are shown. Yields (I$_{rel}$) are shown relative to the state with the highest cross section, the $\frac{1}{2}^+$ at 682.9 keV. New spin/parity and Nilsson label assignments are signified by a star. Some levels of interest which are not directly populated by the reaction, or not detected due to low γ-ray detection efficiency at low energies, are shown for completeness (signified by a dash in the I$_{rel}$ column). Relative yields are measured between 33° and 55° with respect to the beam axis.

E^* (keV)	I$_{rel}$	J^π	$\Omega^\pi[Nn_z\Lambda]$
0.0	-	$\frac{3}{2}^-$	$\frac{3}{2}^-[521]$
54.533 (6)	-	$\frac{5}{2}^-$	$\frac{3}{2}^-[521]$
63.91 (5)	-	$\frac{5}{2}^+$	$\frac{5}{2}^+[642]$
115.717 (7)	-	$\frac{7}{2}^+$	$\frac{5}{2}^+[642]$
131.455 (7)	6.1(7)	$\frac{7}{2}^-$	$\frac{3}{2}^-[521]$
180.229 (9)	-	$\frac{9}{2}^+$	$\frac{5}{2}^+[642]$
227.31 (5)	1.1(2)	$\frac{9}{2}^-$	$\frac{3}{2}^-[521]$
272.25 (21)	2.7(3)	$\frac{11}{2}^+$	$\frac{5}{2}^+[642]$
347.25 (7)	1.5(2)	$\frac{11}{2}^-$	$\frac{3}{2}^-[521]$
361.10 (10)	0.03(1)	$\frac{13}{2}^+$	$\frac{5}{2}^+[642]$
426.60 (5)	-	$\frac{11}{2}^-$	$\frac{11}{2}^-[505]$
434.426 (6)	2.35(24)	$\frac{5}{2}^-$	$\frac{5}{2}^-[523]$
474.629 (6)	63.6(25)	$\frac{3}{2}^+$	$\frac{3}{2}^+[402]$
478.87 (8)	2.0(2)	$\frac{13}{2}^-$	$\frac{3}{2}^-[521]$
514.671 (8)	4.0(4)	$\frac{7}{2}^-$	$\frac{5}{2}^-[523]$
524.850 (7)	2.4(6)	$\frac{5}{2}^+$	$\frac{3}{2}^+[402]$
579.46 (9)	-	$\frac{13}{2}^-$	$\frac{11}{2}^-[505]$
617.48 (3)	1.7(3)	$\frac{9}{2}^-$	$\frac{5}{2}^-[523]$
682.90 (4)	100(4)	$\frac{1}{2}^+$	$\frac{1}{2}^+[400]$
683.233 (9)	-	$\frac{3}{2}^+$	$\frac{3}{2}^+[651]$
729.02 (17)	13.4(9)	$\frac{1}{2}^-$, $\frac{3}{2}^-$*	
793.5 (2)	4.1(3)	$\frac{1}{2}^-$	$\frac{1}{2}^-[530]$
809.0 (2)	33.5(28)	$\frac{3}{2}^-$	$\frac{1}{2}^-[530]$
849.3 (2)	2.43(27)	$\frac{11}{2}^+$, $\frac{13}{2}^+$*	
919.50 (5)	3.9(5)	$\frac{7}{2}^+$	$\frac{1}{2}^+[400]$
1552.2 (2)	3.6(6)	$\frac{5}{2}^+$*	
1563.1 (6)	1.4(4)	$(\frac{3}{2}^-, \frac{5}{2}^-, \frac{5}{2}^+, \frac{7}{2}^-)$*	
1589.8 (2)	4.8(8)	$\frac{3}{2}^+$, $\frac{5}{2}^+$*	
1735.6 (2)	4(1)	$\frac{5}{2}^+$*	
1825.6 (1)	14.3(32)	$\frac{5}{2}^+$*	
1905.9 (4)	4.9(15)	$\frac{11}{2}^-$*	$\frac{9}{2}^-[514]$*

darenko *et al.* detects both the 674 keV and 729 keV γ rays, seen in this work, and assigns the state as a $\frac{3}{2}^-$, $\frac{1}{2}^-$[521] Nilsson candidate which is above the Fermi surface indicated in Fig. 5. Whilst we are not able to make a firm Nilsson configuration assignment we note the moderate relative intensity that we measure and remind the reader that we do not expect to populate levels *above* the

Fermi surface with high intensity by the (p,d) reaction. Upon inspection of Table VII and the Nilsson diagram, Fig.5, the only other $\frac{3}{2}^-$ level which we intensely populate is the $\frac{3}{2}^-$, $\frac{1}{2}^-$[530] at 809 keV. We note that there is not a firm $\frac{3}{2}^-$, $\frac{3}{2}^-$[532] configuration in ^{157}Gd and offer it as an possible alternative candidate for this level.

D. The 1563 state

In addition to the level at 1552 keV discussed above, a second level with transitions to the three lowest lying levels in the ground state band is observed at an excitation energy of 1563.1± 0.6 keV, Table VI. This level is observed with $\sim \frac{1}{3}$ of the intensity of the 1552 keV level, Table VII. This is in agreement with the 1967 (d,t) measurement by Tjøm and Elbek [1], who observed a level at 1569 ± 5 keV with $\sim \frac{1}{5}$ of the intensity of a level at 1556 ± 5 keV. Due to the low statistics, we cannot extract an angular momentum transfer from the deuteron angular distribution for this level. Based upon the observed γ-ray transitions, the J$^\pi$ is narrowed down to either $\frac{3}{2}^-$, $\frac{5}{2}^-$, $\frac{5}{2}^+$ or $\frac{7}{2}^-$.

V. DISCUSSION

The (p,d) reaction employed in the current study is highly-selective, acting like a precision forceps, plucking neutrons from single quasi-neutron orbitals close to and also far below the neutron Fermi surface. The Nilsson diagram, presented in Fig. 5, shows the positions of the neutron orbitals expected to play a role in these (p,d) reactions. Both ^{153}Gd and ^{157}Gd have a $\frac{3}{2}^-$ ground state based on the neutron $\frac{3}{2}^-$[521] orbital (as does the intermediate ^{155}Gd nucleus). The (p,d) reaction employed in the current study should and does predominantly populate quasi-particle states below the $\frac{3}{2}^-$[521] in Fig. 5.

The excitation energy, relative yield, and Nilsson assignments of the levels which are strongly populated in ^{153}Gd and ^{157}Gd are given in Tables V and VII. Similar data for ^{155}Gd, also measured using the (p,d) reaction at 25 MeV, can be found in the study of Allmond *et al.* [12]. In all three isotopes, the $\frac{1}{2}^+$[400] and $\frac{3}{2}^+$[402] band heads are the most strongly populated positive-parity states. The $\frac{5}{2}^+$[402] orbital, newly identified in ^{153}Gd in this work and previously observed in ^{155}Gd, is respectively the fourth and third most intensely populated positive-parity state. In ^{157}Gd, the candidate for the $\frac{5}{2}^+$[402] state is less clear and no firm assignment is made.

For the negative parity levels the $\frac{3}{2}^-$, $\frac{1}{2}^-$[530] level is the most strongly-populated excited state in all three nuclei. In ^{153}Gd the $\frac{5}{2}^-$[523] orbital is also populated with a significant cross section. This orbital is observed at much higher excitation energy in ^{155}Gd and ^{157}Gd and

experiences little direct population.

Partial level schemes for ^{153}Gd, ^{155}Gd and ^{157}Gd, showing every level directly detected following the (p,d) reaction, are presented in Fig. 9. The excitation energies, Nilsson assignments and spherical parent orbitals for key levels in the three isotopes are summarized in Table VIII.

As discussed in our recent publication [28], the most striking feature in Fig. 9 is the gap in the level schemes, $\sim$ 700 keV wide, where no states are populated by the (p,d) reaction. In each case the one-neutron pickup reaction populates a cluster of low lying levels (around $\sim$ 500 keV) and a second group of levels at higher excitation energy ($\sim$ 1500 keV) but nothing in between. This feature is clearly seen in the deuteron spectra in Fig. 10 (reproduced from [28]) where deuterons detected in coincidence with γ rays are shown. The gap in the level schemes corresponds to this trough between the two "peaks" and is visible in all three spectra.

The cluster of levels at low excitation energies originate from the $h_{11/2}$, $d_{3/2}$, and $s_{1/2}$ orbitals from the N = 82 shell and the intruding $h_{9/2}$, $f_{7/2}$, and $i_{13/2}$ orbitals from the N = 126 shell. For moderate deformation these orbitals all lie near the N $\sim$ 90 Fermi surface.

Only two levels above the energy gap (c.f. Fig. 9 and Fig. 10) have been positively assigned. One is based on the negative parity $\frac{9}{2}^-$[514] orbital, the other on the positive parity $\frac{5}{2}^+$[402] orbital. The pseudospin partner of the $\frac{5}{2}^+$[402] orbital, the $\frac{7}{2}^+$[404], is not identified in the current work. In ^{155}Gd, a level was assigned this configuration based upon a combination of new [12] and old [41] data. Experiments to unequivocally locate this configuration in these nuclei, (by imparting slightly higher spin than the (p,d) reaction does), would be beneficial to the following interpretation.

The energy of the $\frac{5}{2}^+$[402] is rapidly up-sloping with increasing deformation. It and its pseudospin partner, the $\frac{7}{2}^+$[404], originate deep below the neutron Fermi surface and from below the N = 64 sub-shell gap. It is the essentially parallel trajectories of these two orbitals and the other pseudospin partners (originating from the $d_{3/2}$, $s_{1/2}$ spherical orbitals) that creates a persistent region of low level density in the Nilsson diagram and which is responsible for the observed gap in the level schemes. This is reminiscent of the situation in high-spin superdeformed nuclei where deformed shell gaps appear near the Fermi surface for certain favored deformations and for certain favored particle numbers.

Thus, the gap in the neutron quasi-particle excitation spectrum in these moderately deformed Gd nuclei owes its origin to the presence of a spherical neutron sub-shell closure at N = 64 (almost 30 neutrons away from these N $\sim$ 90 systems). While the existence of a proton Z = 64 shell gap has become widely accepted [42, 43] the existence or absence of the corresponding N = 64 spherical sub-shell closure has been the subject of ongoing debate in the literature for many years, with arguments going both ways [44–48].

TABLE VIII. Excitation energies (keV) of previously established and presently assigned Nilsson orbital band heads for ^{153}Gd, ^{155}Gd and ^{157}Gd. Those directly populated in this work (or Ref. [12]) are shown in bold.

$\Omega^\pi[Nn_z\Lambda]$	Shell	E* ^{153}Gd	E* ^{155}Gd	E* ^{157}Gd
$\frac{3}{2}^-$[521]	$2f_{7/2}$	**0.0**	**0.0**	**0.0**
$\frac{5}{2}^-$[523]	$2f_{7/2}$	**109.8**	454.5	**434.4**
$\frac{3}{2}^-$[532]	$1h_{9/2}$	**129.2**	287.0	
$\frac{11}{2}^-$[505]	$1h_{11/2}$	171.2	121.1	426.6
$\frac{3}{2}^+$[651]	$1i_{13/2}$	183.5	105.3	683.2
$\frac{3}{2}^+$[402]	$2d_{3/2}$	**212.0**	**268.7**	**474.6**
$\frac{1}{2}^-$[530]	$1h_{9/2}$	**315.2**	451.4	**794**
$\frac{1}{2}^+$[400]	$2d_{3/2}$	**327.9**	**367.7**	**682.9**
$\frac{5}{2}^+$[402]	$2d_{5/2}$	**1152.9**	**1296.1**	$\sim$**1700**
$\frac{7}{2}^+$[404]	$1g_{7/2}$		**752.5**	
$\frac{11}{2}^-, \frac{9}{2}^-$[514]	$1h_{11/2}$	**1474.3**	**1577.9**	**1905.9**

The gadolinium nuclei in question belong to a region of rapid shape change around N = 90. Upon inspection of the neighboring even-even isotopes, low-lying states in ^{152}Gd reveal a predominantly vibrational character, ^{154}Gd is transitional and ^{156}Gd is deformed. However, if the deformation of these odd-mass Gd nuclei tracks that of their even-even partners (from less to more deformed as N increases) one would expect both the excitation energy and width to decrease with neutron number (c.f. Fig. 5). This is the opposite of what is seen experimentally where the orbitals involved are rapidly approaching the Fermi surface ($\frac{3}{2}^-$[521]). A hole in such a deformation driving orbital should polarize the nuclear shape and drive the nucleus to more deformed shapes. The increase in excitation energy of the $\frac{5}{2}^+$[402] with neutron number and ground-state deformation across N = 90, is therefore counterintuitive (cf. Fig. 5).
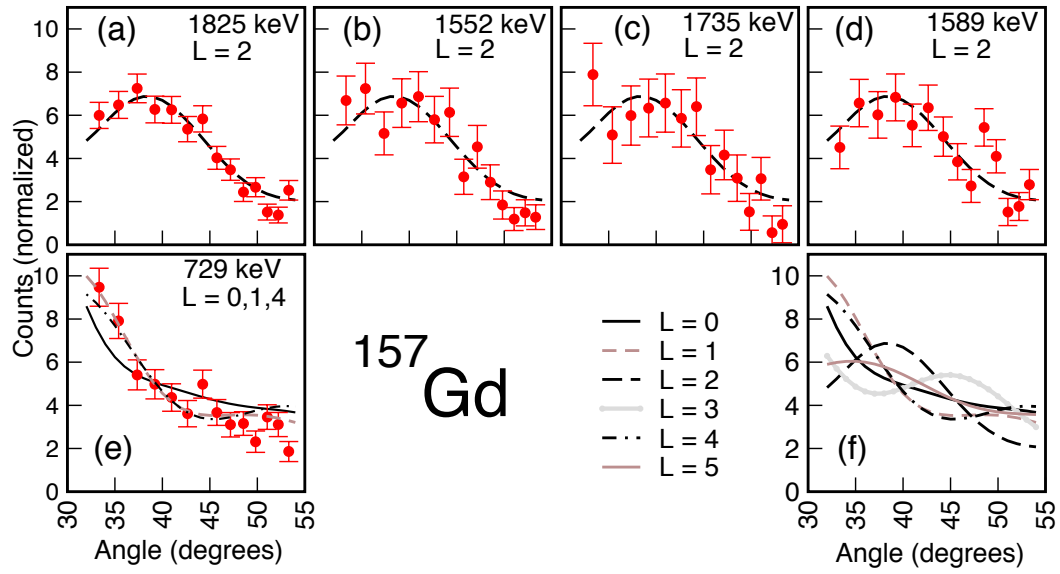
FIG. 8. (Color online.) Angular distributions of deuterons in coincidence with ^{157}Gd states of interest are shown. The state and angular momentum transfer are given in the top right of each panel. The data are the points with error bars. The DWBA calculated curve which best fits the data is also shown in each panel. The calculated curves for $\Delta\ell = 0$ $\hbar$ through $\Delta\ell = 5$ $\hbar$ are shown in the bottom right hand panel.
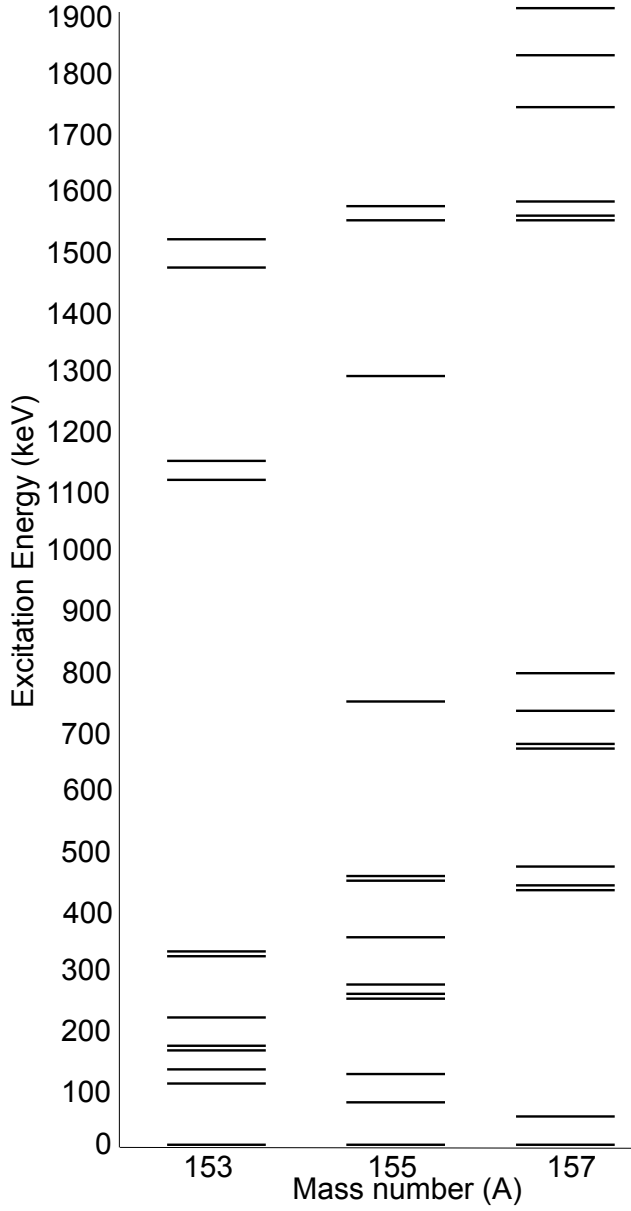
FIG. 10. The deuteron particle projections for the three Gd isotopes. a) ^{154}Gd(p,d-γ)^{153}Gd. b) ^{156}Gd(p,d-γ)^{155}Gd, [12]. c) ^{158}Gd(p,d-γ)^{157}Gd. This figure first appeared in Ref. [28] and is reproduced for easy reference.

FIG. 9. Energy of levels directly populated by the (p,d) reaction are shown for the three Gd isotopes.

VI. SUMMARY AND CONCLUSIONS

A comprehensive study of the low-spin structures of ^{153}Gd and ^{157}Gd has been carried out using a combination of particle and γ-ray detection. The known low-lying, low-spin level structures of both nuclei have been confirmed. Numerous γ rays are observed for the first time and several new quasi-neutron level assignments have been made in both nuclei. Of particular interest is the $\frac{5}{2}^+[402]$ band head identified in ^{153}Gd which follows a similar reassignment in ^{155}Gd, [12]. The location of the $\frac{5}{2}^+[402]$ orbital in ^{157}Gd is less clear, where several states populated with $\Delta\ell = 2\,\hbar$ transfer are observed at ~ 1.7 MeV.

The structure of these odd-N nuclei populated by the (p,d) reaction reveals a large energy gap between ~ 1 and 2 MeV excitation energy. The presence of such a large gap in the excitation spectrum of these N = 90 nuclei indicates the persistence of the N = 64 shell gap,

deep below the Fermi surface, at least to intermediate deformations. It is striking that such an undiluted effect is observed so far below the Fermi surface.

VII. ACKNOWLEDGMENTS

[1] P. O. Tjøm and B. Elbek, Mat. Fys. Medd. K. Dan. Vidensk. Selsk. **36**, 8 (1967).
[2] G. Løvhøiden and D. G. Burke, Can. J. Phys. **51** 2354 (1973).
[3] G. Løvhøiden, D. G. Burke and J. C. Waddington, Can. J. Phys. **51** 1369 (1973).
[4] J. Rekstad *et al.*. Nucl. Phys. **A371** 364 (1981).
[5] K. Yagi *et al.* Nucl. Phys. **A138** 133 (1969).
[6] G. Løvhøiden *et al.* Nucl. Phys. **A160**, 305 (1971).
[7] F. Sterba *et al.*. Nucl. Phys. **A162** 353 (1971).
[8] G. Løvhøiden *et al.* Nucl. Phys. **A494** 157 (1989).
[9] J. Kopecky *et al.* Phys. Rev. C **47**, 1 (1993).
[10] V. Bondarenko *et al.* Nucl. Phys. **A726** 175 (2003).
[11] N. Blasi, S. Micheletti, M. Pignanelli, R. De Leo, A. Gollwitzer, S. Deylitz, B. D. Valnion, G. Graw, and L. A. Malov, Nucl. Phys. **A624** 433 (1997).
[12] J. M. Allmond *et al.* Phys. Rev. C **81**, 064316 (2010).
[13] E. Sheldon. Rev. Mod. Phys. **35**, 795 (1963).
[14] H.J. Rose and D.M. Brink Rev. Mod. Phys. **39**, 306 (1967).
[15] F. Rybicki *et al.* Nucl. Phys. A **146**, 659 (1970).
[16] D.G. Sarantites *et al.* Nucl. Instrum. Meth. A**381**, p.418 (1996).
[17] C.J. Gross *et al.* Nucl. Instrum. Meth. A**450**, p.12 (2000).
[18] S. R. Lesher *et al.* Nucl. Instrum. Meth. A**621**, p.286 (2010).
[19] E. Farnea *et al.* Nucl. Instrum. Meth. A**400**, p.87 (1997).
[20] M. Guttormsen *et al.* Nucl. Instrum. Meth. A**648**, p.168 (2011).
[21] J.A. Cizewski *et al.* Nucl. Instrum. Meth. B**261**, p.938 (2007).
[22] R. Hatarik *et al.* Phys. Rev. C **81**, 011602(R) (2010).

[23] J.J. He *et al.* Phys. Rev. C **80**, 042801(R) (2009).
[24] W.N. Catford *et al.* Phys. Rev. Lett. **104**, 192501 (2010).
[25] K. Wimmer *et al.* Phys. Rev. Lett. **105**, 252501 (2010).
[26] T.J. Ross *et al.* Phys. Rev. C **85**, 051304(R) (2012).
[27] J.M. Allmond *et al.* Phys. Rev. C **86**, 031307(R) (2012).
[28] T.J. Ross *et al.* Phys. Rev. C **88**, 031301(R) (2013).
[29] N.D. Scielzo *et al.* Phys. Rev. C **81** 034608 (2010).
[30] Micron Semiconductor Ltd. (http://www.micronsemiconductor.co.uk)
[31] T. Kibédi *et al.* Nucl. Instrum. Meth. A**589** p.202 (2008)
[32] P.D. Kunz, DWUCK4, University of Colorado (unpublished).
[33] D.G. Fleming, M. Blann, H.W. Fulbright and J.A. Robbins, Nucl. Phys. A **157**, p.1 (1970).
[34] C.M. Perey and F.G. Perey, Phys. Rev. **132**, 755 (1963)
[35] C.M. Perey and F.G. Perey, Atomic Data and Nuclear Data Tables **17**, 1-101 (1976).
[36] R. G. Helmer. Nucl. Data Sheets **107**, 507 (2006).
[37] B.A. Alikov *et al.* Nucl. Phys. **A383** 333 (1982).
[38] A. Spits *et al.* BLG 703 (1996), edited by A.Spits and P.H.M.Van Assche.
[39] R. G. Helmer. Nucl. Data Sheets **103**, 565 (2004).
[40] J. Borggreen *et al.* Nucl. Phys. **A95** 95 (1967).
[41] H.H. Schmidt *et al.* J. Phys. G **12** 411 (1986).
[42] R.R. Chasman Phys. Rev. C **21**:456-458 1 (1980).
[43] P. Mukherjee, R. Bhattacharya and I. Mukherjee Phys. Rev. C **24**:1810-1811 4 (1981).
[44] T. Sumikama *et al.* Phys. Rev. Lett. **106**, 202501 (2011).
[45] H. Hua *et al.* Phys. Rev. C **69** 014317 (2004).
[46] C. Piller *et al.* Phys. Rev. C **42** 182 (1990).
[47] V.R. Green *et al.* Phys. Lett. B **173** 2 (1986).
[48] R. Wenz, A. Timmermann and E. Matthias Z. Phys. A **303** 2 (1981).